

See discussions, stats, and author profiles for this publication at: <https://www.researchgate.net/publication/319631436>

Development and characterization of polyvinyl alcohol stabilized polylactic acid/ZnO nanocomposites

Article in *Materials Research Express* · September 2017

DOI: 10.1088/2053-1591/aa8b8d

CITATION

1

READS

111

6 authors, including:



Ivan Restrepo

Leitat Technological Center

2 PUBLICATIONS 1 CITATION

SEE PROFILE

Some of the authors of this publication are also working on these related projects:



Evaluación de la influencia del cobre y el níquel en la cinética de corrosión de los aceros autoprotectores por espectroscopía de impedancia in situ y ex situ [View project](#)

Materials Research Express



PAPER

Development and characterization of polyvinyl alcohol stabilized polylactic acid/ZnO nanocomposites

RECEIVED
7 August 2017

REVISED
27 August 2017

ACCEPTED FOR PUBLICATION
11 September 2017

PUBLISHED
16 October 2017

I Restrepo^{1,2}, N Benito³, C Medinam⁴, R V Mangalaraja¹, P Flores^{1,4} and S Rodríguez-Llamazares⁵

¹ Materials Engineering Department, University of Concepción, Edmundo Larenas 270, Concepción, Chile

² Technological Development Unit, University of Concepción, Avda. Cordillera 2634, Coronel, Chile

³ Faculty of Physical and Mathematics Sciences, Surfaces and Nanomaterials Laboratory, University of Chile, Blanco Encalada 2008, Santiago, Chile

⁴ Mechanical Engineering Department, University of Concepción, Edmundo Larenas 219, Concepción, Chile

⁵ Laboratory Building CIPA, Research Center of Advanced Polymers, Av. Collao 1202, Concepción, Chile

E-mail: s.rodriguez@cipachile.cl (S Rodríguez-Llamazares) and pfloresv@udec.cl (P Flores)

Keywords: melt blending, polylactic acid, ZnO nanoparticles, nanocomposites

Supplementary material for this article is available [online](#)

Abstract

The present work is focused on the development of polylactic acid/ZnO (PLA/ZnO) polymer nanocomposite through a melt blending route. Previously, the ZnO nanoparticles were coated with polyvinyl alcohol (PVA) via a solvothermal method. The morphology of PVA coated ZnO nanostructures and the formation of polymer nanocomposites were identified through transmission electron microscopy analysis. Thermogravimetric analysis showed that PVA coated ZnO(c) nanoparticles incorporated into the PLA matrix exhibited better thermal stability, suggesting that PVA could be acting as a strong stabilizing agent for ZnO nanoparticles. The tensile strength, elastic modulus, strain at maximum strength and the maximum strain were extracted through stress–strain relations.

1. Introduction

Poly(lactic acid) (PLA) is one of the most important synthetic biodegradable thermoplastic polyester polymers which are produced from renewable-based monomers mainly derived from corn starch, tobacco routes and sugarcane [1]. PLA has numerous interesting physical properties including desirable thermal stability, easy processability, low environmental impact and good mechanical properties [2]. The United State Food and Drug Administration (FDA) declared PLA as generally recognized as safe (GRAS) which makes it a promising potential material for biomedical and food packaging industries [3, 4]. Specifically, PLA has been widely used in food packaging containers for fresh fruit and vegetables [5, 6].

Until now, there are reports available on the physical properties but still there is a lack of information on the physical properties for various potential applications [7]. The physical properties of PLA could be improved through several approaches including blending with biopolymers, synthetic polymers [8–10], and the incorporation of finely dispersed nanoparticles to utilize in various technological applications [12–14]. ZnO is a II–VI oxide semiconductor and is extensively used in various technological fields like medicine, environmental science and packaging applications due to its excellent antimicrobial activities [11, 15, 16]. The incorporation of ZnO nanoparticles into the polymer matrix yields an excellent packaging material since it prevents bacterial growth on the materials. Recent years, ZnO incorporated PLA polymers received considerable attention due to their excellent physical and antimicrobial properties which make these materials potential applications in the packaging industry [17].

To date, different routes have been developed for the fabrication of PVA/ZnO nanocomposites, among which the melt blending route is a relatively simple and efficient method to produce PLA/ZnO nanocomposites [11, 18]. Although ZnO acts as a catalyst in the depolymerization, PLA leads to intensive degradation of PLA chains which results in a reduction of the thermomechanical properties of the resultant nanocomposites. To overcome this issue, surface treatment of ZnO nanoparticles is the simplest way to improve the thermomechanical proper-

Table 1. Sample code with corresponding concentration of the constituents of nanocomposites.

Sample code	Ratio PLA/ZnO (wt. %)		
	PLA	ZnO (covered with PVA)	ZnO
PLA—1% ZnO(c)	99	1	
PLA—3% ZnO(c)	97	3	
PLA—5% ZnO(c)	95	5	
PLA—1% ZnO	99		1
PLA—3% ZnO	97		3
PLA—5% ZnO	95		5

ties and PVA has been considered as the best stabilizing agent for ZnO nanoparticles to make the surface treatment [19]. To the best of our knowledge, studies on thermomechanical properties of nanocomposites using PVA as a stabilizing agent for ZnO nanoparticles into a PLA matrix has not yet been reported.

Owing to the importance of PLA/ZnO nanocomposites in various technological industries, in the present work we propose a method for the fabrication of PLA/ZnO nanocomposites using PVA covered ZnO nanoparticles. The structural and thermomechanical properties of the PLA/ZnO nanocomposites are reported.

2. Experimental

2.1. Materials

The commercial PLA grade 3251D, Mw of 55.4 kg mol⁻¹ and isomer D lactic acid content of 1.2% [20] was purchased from Nature Works[®], United States. Powder of Zinc Oxide nanoparticles, with particle size lower than 100 nm, were provided by Sigma Aldrich[®]. PVA with hydrolysis degree 87–89% and molecular weight 85–124 (kg mol⁻¹) were provided by Sigma Aldrich[®]. The neat PLA processed under similar conditions was studied as a reference material. All reagents used in these experiments were of high purity.

2.2. Processing

The PLA/ZnO nanocomposites were prepared via melt processing in a Brabender mixer (Plastograph[®] EC plus, Mixer 50EHT32, Germany) at 60 rpm for 8 min and the temperature was kept at 190 °C. The PLA was dried at 40 °C overnight in a vacuum oven.

Initially, for the surface modification of ZnO nanoparticles, PVA and ZnO with a ratio of 10:1 were dispersed in double distilled water and kept at constant stirring for 24 h at 70 °C. The resulting mixture was then centrifuged at 5000 rpm for 2 h. In order to remove excess PVA, the resulting mixture was re-dispersed in ethanol and kept under a sonication process and further centrifuged at 5000 rpm for 2 h. The obtained PVA covered ZnO particles were dried in an oven at 80 °C for 12 h and is denoted as ZnO(c).

Later, the PLA/ZnO(c) nanocomposites were prepared with different concentrations of 1, 3 and 5 wt. % ZnO(c) nanoparticles (see table 1). Then the composites were poured into the melt blending equipment. The obtained nanocomposites were pressure-molded at 30 bar, 190 °C and 10 min in order to obtain plates for x-ray diffraction (XRD) analysis. In addition, PLA/ZnO nanocomposite was prepared using PVA uncovered ZnO nanoparticles for comparison.

2.3. Nanocomposite characterization

Thermal stability of the nanocomposites was evaluated using a thermogravimetric analyzer Netzsch TGA 209 F3 (Tarsus, Selb, Germany). Thermogravimetric analysis (TGA) scans were carried out at 10 °C min⁻¹ under nitrogen atmosphere (20 ml min⁻¹), in the temperature range between 35 and 600 °C. The following parameters were extracted from the TGA data: (i) temperature at maximum decomposition rate (T_{max}), (ii) weight loss associated with T_{max} (WL T_{max}), (iii) the onset temperature (T_{onset}) corresponding to each decomposition step and (iv) the temperature corresponding to 5% weight loss ($T_{5\%}$).

The XRD measurements were recorded on a Bruker diffractometer endeavor model D4/MAX-B (United States) operated at 40 kV, 20 mA, at room temperature, using a CuK α source with the wavelength of $\lambda = 1.5405 \text{ \AA}$. The measurements were made with an XRD angle (2θ) in the range of 3–70° with 0.02° step size and a scanning rate of 1° min⁻¹. The neat PLA and PLA/ZnO nanocomposites were previously annealed for 20 min at 120 °C under vacuum conditions.

X-ray photoelectron spectroscopy (XPS) spectra were measured using a hemispherical analyser (Physical Electronics 1257 system). A twin anode (Mg and Al) x-ray source was operated at a constant power of 200 W using Al K α radiation (1486.6 eV). The sample was placed in a sample stage in which the emission angle can be varied. The emission angle was fixed at 45°.

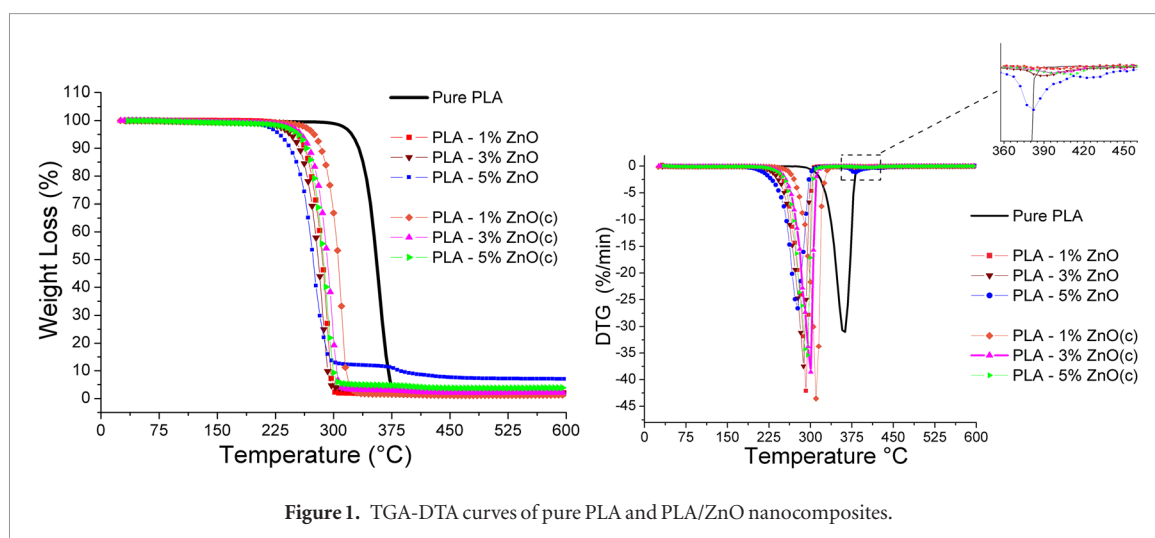


Figure 1. TGA-DTA curves of pure PLA and PLA/ZnO nanocomposites.

Table 2. TGA and DTA parameters of pure PLA, and PLA/ZnO nanocomposites.

Sample	TGA $T_{5\%}$	DTG					
		$T_{\text{onset-1}}$ (°C)	$T_{\text{max-1}}$ (°C)	WL-1 (%)	$T_{\text{On set-2}}$ (°C)	$T_{\text{max-2}}$ (°C)	WL-2 (%)
Pure PLA	334	284	364	99	—	—	—
PLA—1% ZnO(c)	284	235	310	98	380	410	0.3
PLA—3% ZnO(c)	269	200	301	96	370	396	0.7
PLA—5% ZnO(c)	265	200	295	94	375	410	0.8
PLA—1% ZnO	252	182	292	98	377	401	0.2
PLA—3% ZnO	243	182	287	96	377	387	0.8
PLA—5% ZnO	228	167	277	87	367	382	2.5

The mechanical properties of PLA/ZnO nanocomposites were evaluated using tensile tests performed on a Instron 8801 universal testing machine according to ASTM D638 standards. Prior to the measurements, the specimens were stored at 25 °C and 65% relative humidity (HR) for 7 d. The crosshead speed was set at 10 mm min⁻¹. The Young's modulus, strength, and elongation percentage at break were obtained from the stress-strain curves. At least 5 individual measurements were carried out for each formulation and the mean values and standard deviations were reported. The collected data were evaluated with a one-way analysis of variance at the 95% confidence level.

Transmission electron microscopy (TEM) images of the nanocomposites were obtained using a trademark FEI model Tecnai G2 F20 S-Twin, equipped with an electron gun of 2 (Å) diameter, operated at a tension of 120 kV and extraction voltage of 3400 V. The magnifications used were 100× and 500×.

3. Results and analysis results

3.1. TGA analysis

TGA analysis of pure PLA and PLA/ZnO nanocomposites is shown in figure 1 and the extracted values of thermal parameters are summarized in table 2. The TGA curve for pure PLA (figure 1) showed one-step decomposition with a weight loss of 99% associated with the loss of ester groups by unzipping depolymerization [21, 22]. T_{max} for pure PLA was 364 °C. In contrast, PLA/(ZnO(c)-ZnO) nanocomposites displayed two degradation steps (see figure 1), the first one, around 170–330 °C with weight loss ranged from 87.3 to 98%, which is related to the decomposition step of PLA close to ZnO surface. The second step, between 367–425 °C could be associated with the degradation of PLA that is far from nanoparticles [23].

The addition of covered and uncovered ZnO nanoparticles to PLA, leads to a reduction in thermal stability of the polymeric matrix which is in direct correlation with the concentration of nanoparticles, therefore, as the ZnO content increases, the thermal stability for PLA decreases. However, PLA/ZnO nanocomposites containing uncovered ZnO nanoparticles presented a more intensive reduction in $T_{5\%}$ and $T_{\text{max-1}}$, in comparison with those containing covered nanoparticles.

It is reported for polymer nanocomposites that the addition of ZnO to various polymer matrices can lead to either stabilizing or degradation effects [11]. In the present case, nanocomposites containing ZnO nanoparticles covered with PVA exhibited better thermal stability than those containing uncovered nanoparticles. The nature

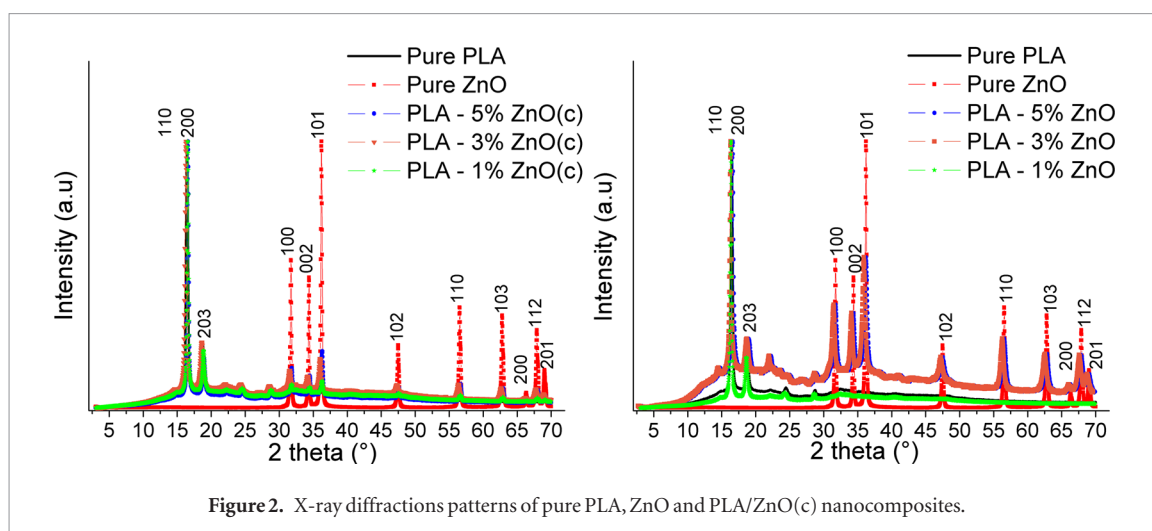


Figure 2. X-ray diffractions patterns of pure PLA, ZnO and PLA/ZnO(c) nanocomposites.

of partial compatibility between PVA and PLA favoring intramolecular entanglement between them [9, 24, 25]. In this context PVA could be acting as a stabilizing agent for ZnO nanoparticles, diminishing its catalytic action on the polymeric matrix. As a result, higher thermal stability of PLA/ZnO(c) nanocomposites is observed in comparison with uncovered nanoparticles.

3.2. XRD results

The XRD patterns for pure PLA, ZnO and PLA/ZnO(c) nanocomposites are shown in figure 2. Two characteristic peaks located at 16.5 and 18.8° correspond to the (110)/(200) and 203 planes with two chains in a helical conformation which confirmed that the pure PLA is in a pseudo-orthorhombic α -phase crystallite structure [26, 27]. In addition to PLA diffraction peaks, the characteristic peaks of ZnO were also identified indicating the presence of the nanoparticles in the nanocomposites. The most intense peaks were observed at around 32 and 36° which correspond to the planes of hexagonal wurtzite structure of ZnO. Moreover, the diffraction patterns of PLA/ZnO nanocomposites did not show any changes in the full width at half maximum and peak position compared with the pure PLA, confirming that the presence of covered and uncovered ZnO nanoparticles does not alter the semi-crystalline nature of PLA structures. These results are consistent with reports in literature indicating that crystallinity of the polyester matrix can be enhanced with the addition of ZnO nanoparticles, because the crystalline phases of PLA present a greater resistance to the hydrolytic degradation exerted by ZnO nanoparticles, in regard to amorphous ones. Thus, as a result of the progressive shortening of the chain during the hydrolytic degradation, the highly ordered crystalline phase is increased due to a decrease in the molecular entanglement along with a greater mobility of the chain [11, 23].

3.3. XPS analysis

The XPS measurements performed to identify the elemental composition and oxidation state of elements and the XPS spectra of PLA/ZnO nanocomposites with 3 and 5 wt. % of ZnO(c) are shown in figure 3. It can be seen that C, O, Si and a very small contribution of Zn are present in the nanocomposites. In addition to these bands, F related peaks are observed in PLA-5% ZnO(c). In general, fluorine and silicon will be considered as contamination incorporated during the manipulation and processing of the samples.

The high resolution XPS spectra of Zn 2p_{3/2} and Zn L₃M_{3,4}M_{3,4} bands have been measured. Zn 2p_{3/2} band does not provide enough information about the chemical state of zinc due to the small difference in binding energy between Zn⁰ and Zn²⁺ (only 0.3 eV) state [28].

Nevertheless, the determination of the Zn chemical state can be done using the Auger Transition Zn L₃M_{3,4}M_{3,4} and the modified Auger parameter, α' given by equation (1) [29]:

$$\alpha' = BE(\text{Zn } 2p_{3/2}) + KE(\text{Zn } L_3M_{3,4}M_{3,4}). \quad (1)$$

In this case, modified Auger parameters, α' , are 2009.7 and 2009.6 eV, for PLA/ZnO nanocomposites with 3 and 5 wt. % of ZnO nanoparticles, respectively (figure 4). These values are in good agreement with the characteristic value of 2009.8 eV reported for bulk tetrahedral ZnO [28]. The small shifts (0.1–0.2 eV) in the modified Auger parameter are due to interface and size effects, related with the presence of nanoparticles [30, 31].

3.4. Tensile test

The characteristic stress–strain curves are shown in figure 5. It is possible to identify a mechanical behavior for pure PLA exhibiting a plastic deformation, however, this behavior changed from ductile to fragile when ZnO(c) and ZnO nanoparticles were incorporated to the polymeric matrix.

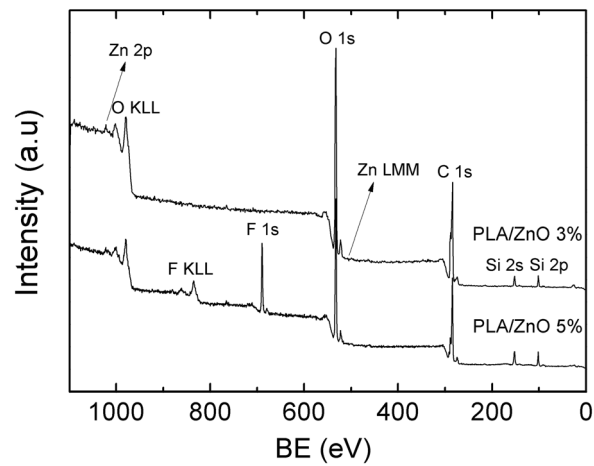


Figure 3. XPS survey spectra of PLA/ZnO nanocomposites with 3 and 5 wt. % of ZnO nanoparticles.

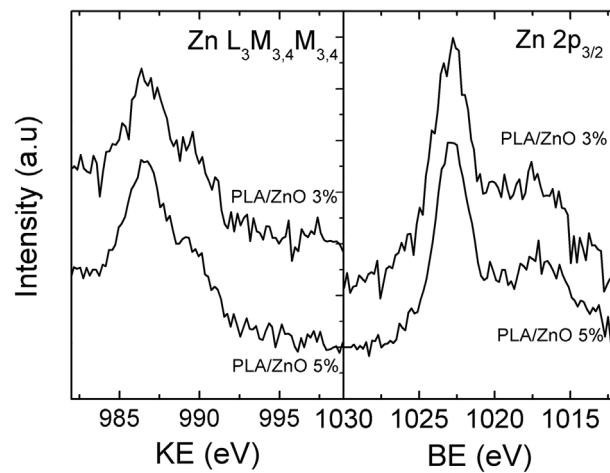


Figure 4. High resolution XPS spectra of Zn $L_{3,4}M_{3,4}$ and Zn $2p_{3/2}$ bands used to calculate modify Auger parameter.

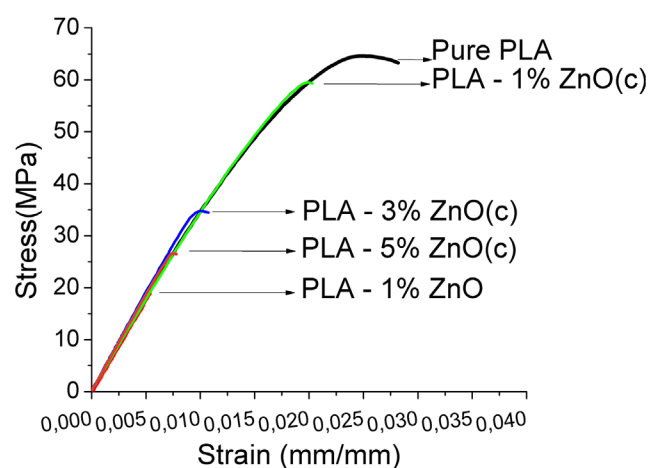
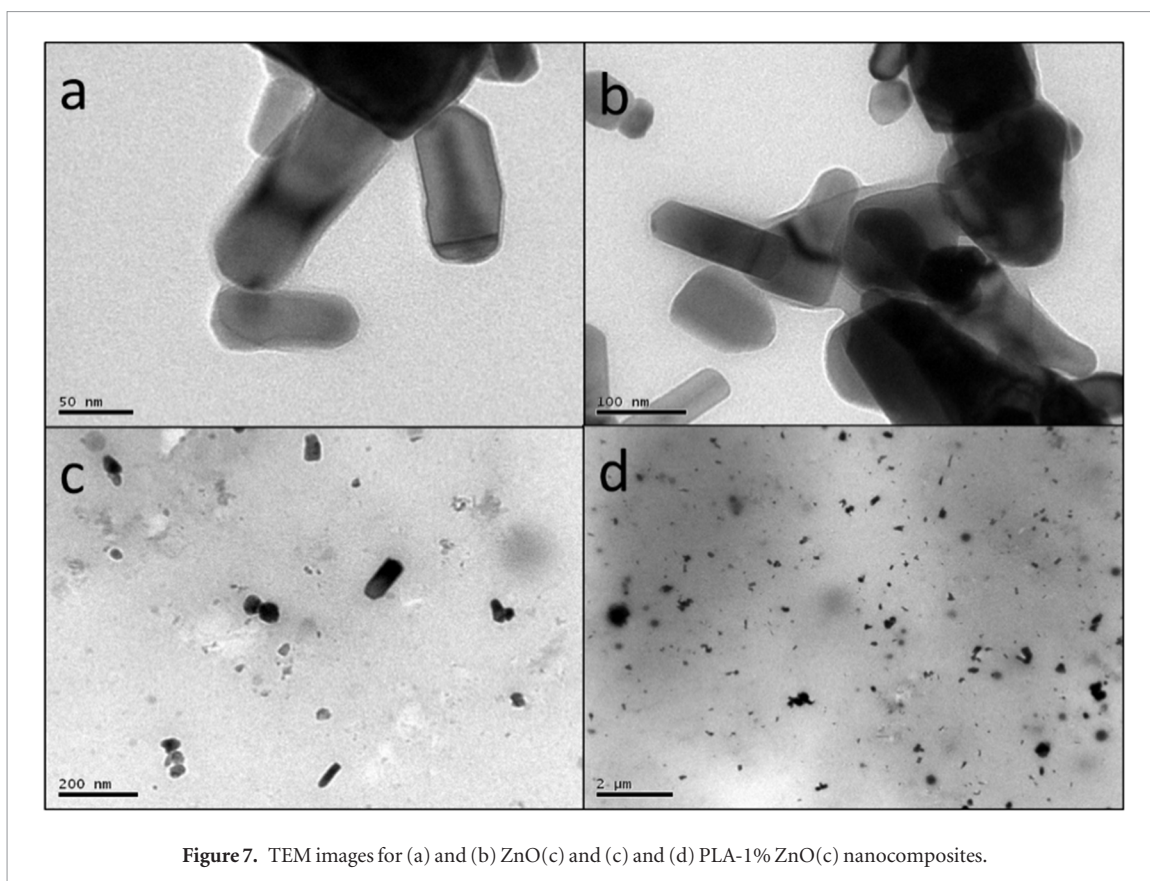
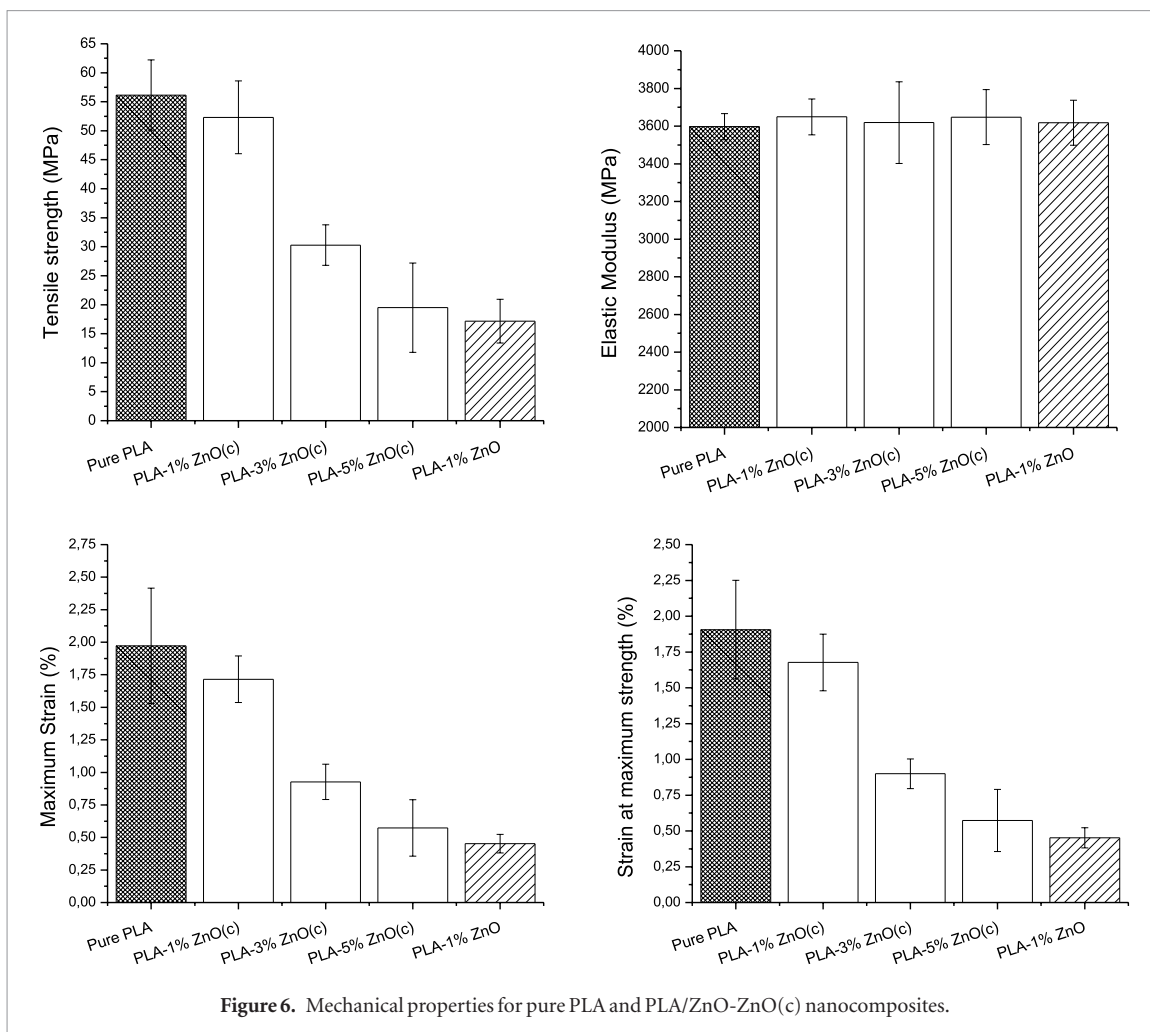


Figure 5. Stress-strain curves for pure PLA and PLA/ZnO nanocomposites.

The tensile strength, elastic modulus, strain at maximum strength and maximum strain for pure PLA, PLA/ZnO(c) and PLA/ZnO nanocomposites are shown in figure 6. The ZnO(c) nanoparticles incorporated nanocomposites exhibited better mechanical properties than the uncovered ZnO nanoparticles. When comparing with pure PLA, the nanocomposites containing 1 wt. % of ZnO(c), do not yield significant changes in the tensile strength, strain at maximum strength and maximum strain as opposed to those with 1 wt. % of ZnO nanoparticles. Nevertheless, by increasing the content of ZnO(c) nanoparticles, the mechanical properties decrease



gradually. Interestingly, the obtained Young's modulus values are almost similar in pure PLA and PLA/ZnO(c)-ZnO nanocomposites.

For nanocomposites PLA-5% ZnO(c), similar values are observed in the elastic modulus compared to the pure PLA due to the stabilization exerted by PVA on the surface of the nanoparticles, favoring PLA/ZnO interfacial interactions and avoiding agglomerations of nanoparticles. Additionally, nanocomposites PLA-1% ZnO, PLA-1% ZnO(c) and PLA-3% ZnO(c) present similar values for elastic modulus in comparison with pure PLA.

It has been reported that for rigid polymers exhibiting elastic modulus of higher than 2.0 GPa, the addition of a low percentage of nanoparticles (below 3 wt. %) produces no influence on the elastic modulus of the nanocomposites due to a low interaction between the nanoparticles and the polymer matrix; however, it can be considerably increased up to 40% with the addition of 5 wt. % of ZnO nanoparticles [32–34].

The addition of ZnO nanoparticles to PLA matrix may induce a more fragile nature to the nanocomposites which yield low tensile strength. This is due to the high susceptibility of the PLA matrix of thermal and hydrolytic degradation in the presence of ZnO nanoparticles [35].

The interface interactions between matrix and filler in nanocomposites are in direct correlation with the mechanical properties and found that PVA covered ZnO nanoparticles incorporated in the PLA matrix exhibited better tensile strength as compared with uncovered ZnO nanoparticles incorporated in the PLA matrix [11]. This is mainly due to PVA being well connected by hydrogen bonding with ZnO nanoparticles [36, 37].

On the other hand, the partial compatibility between PVA and PLA [38], increases the strength of bonding and interfacial interaction, which improve the mechanical properties of PLA/ZnO nanocomposites, due to better stress transference. However, a decrease in tensile strength observed for covered ZnO nanoparticles is associated with the agglomerations of ZnO nanoparticles produced by the PVA covering and creating defects that act as stress concentrators.

3.5. TEM results

TEM images for ZnO(c) nanoparticles and PLA-1% ZnO(c) nanocomposites are presented in figure 7. The micrographs clearly show that PVA successfully covered the ZnO surface and the existence of rod shaped ZnO nanostructures. TEM image of the PLA/ZnO(c) nanocomposite showed that the ZnO particles are distributed in the PLA matrix, however, some points of agglomerations of covered nanoparticles were also identified.

4. Conclusions

In summary, nanocomposites of Poly(lactic acid): ZnO (PLA/ZnO) nanostructures were successfully fabricated through a melt blending route. The morphology of ZnO nanostructures and formation of polymer nanocomposite were identified through TEM images. The TGA and mechanical properties analyses revealed that PVA coated ZnO(c) nanoparticles incorporated PLA/ZnO nanocomposites exhibited better thermal stability and mechanical properties, suggesting that PVA could be acting as a strong stabilizing agent for ZnO nanoparticles.

Acknowledgment

The autor I R would like to thank the CONICYT (Beca de Doctorado Nacional—Proyecto PAI 781411004); CONICYT-REGIONAL Grant No.: PRFC0002—CIPA; Programa de Financiamiento Basal para Centros Científicos y Tecnológicos de Excelencia (Grant No.: PFB-27). The authors thank to Carmen Pradenas for sample testing.

Compliance with ethical standards

Conflict of interest

The authors declare that they have not conflict of interest.

References

- [1] Noroozi N 2013 Rheology and processing of biodegradable poly(caprolactone) polyesters and their blends with polylactides *PhD Thesis* (The University of British Columbia)
- [2] Carrasco F, Pagès P, Gámez-Pérez J, Santana O O and MasPOCH M L 2010 Processing of poly (lactic acid): Characterization of chemical structure, thermal stability and mechanical properties *Polym. Degrad. Stab.* **95** 116–25
- [3] Jamshidian M, Tehrani E A, Imran M, Jacquot M and Desobry S 2010 Poly-lactic acid: production, applications, nanocomposites, and release studies *Compr. Rev. Food Sci. Food Saf.* **9** 552–71
- [4] FDA 2002 *Inventory of Effective Food Contact Substance (FCS), notification No.178* Access date: May 2017 (<https://www.accessdata.fda.gov/scripts/fdc/?set=FCN&id=178>)

- [5] Auras R, Harte B and Selke S 2004 An overview of polylactides as packaging materials *Macromol. Biosci.* **4** 835–64
- [6] Lim R-T, Auras R and Rubino M 2008 Processing technologies for poly (lactic acid) *Prog. Polym. Sci.* **33** 820–52
- [7] Wang L, Ma W, Gross R A and McCarthy S P 1998 Reactive compatibilization of biodegradable blends of poly (lactic acid) and poly(ϵ -caprolactone) *Polym. Degrad. Stab.* **59** 161–8
- [8] Shuai X, He Y, Asakawa N and Inoue Y 2001 Miscibility and phase structure of binary blends of poly (L-lactide) and poly (vinyl alcohol) *J. Appl. Polym. Sci.* **81** 762–72
- [9] Thais M C, de Carvalho R A, Sobral P J, Habitante A M and Solorza-Feria J 2008 The effect of the degree of hydrolysis of the PVA and the plasticizer concentration on the color, opacity, and thermal and mechanical properties of films based on PVA and gelatin blends *J. Food Eng.* **87** 191–9
- [10] Zhang R, Xu W and Jiang F 2012 Fabrication and characterization of dense Chitosan/polyvinyl-alcohol/poly-lactic-acid blend membranes *Fiber Polym.* **13** 571–5
- [11] Murariu M, Doumbia A, Bonnaud L, Dechief A L, Paint Y, Ferreira M, Campagne C, Devaux E and Dubois P 2011 High-performance polylactide/ZnO nanocomposites designed for films and fibers with special end-use properties *Biomacromolecules* **12** 1762–71
- [12] Tankhiwale R and Bajpai S K 2012 Preparation, Characterization and antibacterial applications of ZnO-nanoparticles coated polyethylene films for food packaging *Colloids Surf. B* **90** 16–20
- [13] Prasada V, Shaikha A J, Kathea A A, Bisoyib D K and Vermac A K 2010 Vigneshwarana N. Functional behaviour of paper coated with zinc oxide-soluble starch nanocomposites *J. Mater. Process. Technol.* **210** 1962–7
- [14] Demir M M, Memesa M, Castignolles P and Wegner G 2006 PMMA/Zinc oxide nanocomposites prepared by *in situ* Bulk polymerization *Macromol. Rapid Commun.* **27** 763–70
- [15] Perez P J, Ferreira N, Teofilo R, DosReis J, Vitor D, Batista R A, Olavo S, de Andrade N and Alves E A 2010 Physical-mechanical and antimicrobial properties of nanocomposite films with pediocin and ZnO nanoparticles *Carbohydr. Polym.* **94** 199–208
- [16] FDA 2011 *Substances generally recognized as safe Part 182* Access date: May 2017 (<https://www.accessdata.fda.gov/scripts/cdrh/cfdocs/cfcfr/CFRSearch.cfm?CFRPart=182>)
- [17] Thirumavalavan M, Huang K-I and Lee J-F 2013 Colloids and surfaces a: synthesis and properties of nano ZnO using polysaccharides as chelating agents: effects of various parameters on surface modification of polysaccharides *Physicochem. Eng. Asp.* **417** 154–60
- [18] Therias S, Larche J E, Bussiere P-O, Gardette J I, Murariu M and Dubois P 2012 Photochemical behavior of polylactide/ZnO nanocomposite films *Biomacromolecules* **13** 3283–91
- [19] Bussiere P O, Therias S, Gardette J-L, Murariu M, Dubois P and Baba M 2012 Effect of ZnO nanofillers treated with triethoxy caprylylsilane on the isothermal and non-isothermal crystallization of poly (lactic acid) *Phys. Chem. Chem. Phys.* **14** 12301–8
- [20] Jazrawi B, Noroozi N, Ansari M and Hatzikiriakos S G 2013 Processing aids for biodegradable polymers *J. Appl. Polym. Sci.* (<https://doi.org/10.1002/app.38562>)
- [21] Tsuji H 2005 Poly(lactide) stereocomplexes: formation, structure, properties, degradation, and applications *Macromol. Biosci.* **5** 569–97
- [22] Nalbandi A 2001 Archive of SID kinetics of thermal degradation of polylactic acid under N₂ atmosphere *Iran. Polym. J.* **10** 371–6
- [23] Lizundia E, Ruiz-Rubio L, Vilasab J L and Leonab L M 2016 Towards the development of eco-friendly disposable polymers: ZnO-initiated thermal and hydrolytic degradation in poly(L-lactide)/ZnO nanocomposites *R. Soc. Chem. Adv.* **6** 15660
- [24] Peng Z and Kong L X 2007 A thermal degradation mechanism of polyvinyl alcohol/silica nanocomposites *Polym. Degrad. Stab.* **92** 1061–71
- [25] Alexy P, Bakos D, Crkonova G, Kolomaznik K and Krsiak M 2001 Blends of Polyvinyl alcohol with collagen hydrolysate: thermal degradation and processing properties *Macromol. Symp.* **170** 41–9
- [26] Yeh J-T, Yang M-G, Wu C-H, Wu X and Wu C-S 2008 Study on the crystallization kinetic and characterization of poly (lactic acid) and poly(vinyl alcohol) blends *Polym.-Plast. Technol. Eng.* **47** 1289–96
- [27] Tabatabaei S H and Ajji A 2011 Crystal structure and orientation of uniaxially and biaxially oriented PLA and PP nanoclay composite films *J. Appl. Polym. Sci.* **124** 4854–63
- [28] Biesinger M C, Lau L W M, Gerson A R and Smart R 2010 Resolving surface chemical states in XPS analysis of first row transition metals, oxides and hydroxides: Sc, Ti, V, Cu and Zn *Appl. Surf. Sci.* **257** 887–98
- [29] Martin-Concepción A I, Yubero F, Espinos J P, González-Elipe A R and Tougaard S 2003 X-ray photoelectron spectroscopy study of the first stages of ZnO growth and nanostructure dependence of the effects of polarization at ZnO/SiO₂ and ZnO/Al₂O₃ interfaces *J. Vac. Sci. Technol. A* **21** 1393
- [30] Lassaletta G, Fernandez A, Espinos J P and Gonzalez-Elipe A R 1995 Spectroscopic characterization of quantum-sized TiO₂ supported on silica: influence of size and TiO₂-SiO₂ interface composition *J. Phys. Chem.* **99** 1482–90
- [31] Espinos J P, Morales J, Barranco A, Caballero A, Holgado J P and Gonzalez-Elipe A R 2002 Interface Effects for Cu, CuO and Cu₂O Deposited on SiO₂ and ZrO₂, XPS determination of the valence state of copper in Cu/SiO₂ and Cu/ZrO₂ catalysts *J. Phys. Chem. B* **106** 6921–9
- [32] Ci L and Bai J 2006 The reinforcement role of carbon nanotubes in epoxy composites with different matrix stiffness *Compos. Sci. Technol.* **66** 599–603
- [33] Pantani R, Gorrasi G, Vigliotta G, Murariu M and Dubois P 2013 PLA-ZnO nanocomposite films: Water vapor barrier properties and specific end-use characteristics *Eur. Polym. J.* **49** 3471–82
- [34] De Silva R T, Pasbakhsh P, Lee S M and Kit A Y 2015 ZnO deposited/encapsulated halloysite-poly (lactic acid)(PLA) nanocomposites for high performance packaging films with improved mechanical and antimicrobial properties *Appl. Clay Sci.* **111** 10–20
- [35] Raquez J M, Habibi Y, Murariu M and Dubois P 2013 Polylactide (PLA)-based nanocomposites *Prog. Polym. Sci.* **38** 1504–42
- [36] Kumar N B, Crasta V and Praveen B M 2014 Advancement in microstructural, optical, and mechanical properties of PVA (Mowiol 10-98) doped by ZnO nanoparticles *Phys. Res. Int.* **2014** 1–9
- [37] Nabiyouni G, Barati A and Saadat M 2011 Surface adsorption of polyethylene glycol and polyvinyl alcohol with variable molecular weights on zinc oxide nanoparticles *Iran. J. Chem. Eng.* **8** 21
- [38] Thomas S, Grohens Y and Jyotishkumar P (ed) 2014 *Characterization of Polymer Blends: Miscibility, Morphology and Interfaces* (New York: Wiley)